PERGAMON

International Journal of Heat and Mass Transfer 42 (1999) 4259–4273

International Journal of HEAT and MASS TRANSFER

www.elsevier.com/locate/ijhmt

An inverse natural convection problem of estimating the strength of a heat source

H.M. Park*, O.Y. Chung

Department of Chemical Engineering, Sogang University, Shinsoo-Dong, Mapo-Gu, Seoul, South Korea

Received 20 October 1998; received in revised form 18 March 1999

Abstract

The inverse problem of determining the time-varying strength of a heat source, which causes natural convection in a two-dimensional cavity, is considered. The Boussinesq equation is used to model the natural convection induced by the heat source. The inverse natural convection problem is posed as a minimization problem of the least-square criterion, which is solved by a conjugate gradient method employing the adjoint equation to determine the descent direction. The present method solves the inverse natural convection problem accurately without any simplification of the governing Boussinesq equation.

1. Introduction

The aim of the present work is to determine the unknown strength of a time-varying heat source, which causes natural convection in a cavity, based on temperature measurement in the domain. If the strength of the heat source is known, one solves the Boussinesq equation containing a heat source term to obtain the velocity and temperature field. This is the direct problem. On the contrary, the strength of the heat source can be determined with the help of extra conditions such as temperature measurements at the interior points of the domain. Such a problem is called an inverse problem and can be regarded as discovering the cause from a known result. The inverse heat transfer problems have numerous applications in various branches of science and engineering, but the solution of inverse problems is not straightforward due to their ill-posedness in the sense of Hadamard: small perturbations in the observed functions may result into large changes in the corresponding solutions [1–3]. The ill-posed nature renders many algorithms used for direct problems inapplicable to inverse problems, and special numerical techniques must be employed to stabilize the results of calculations. Commonly adopted technique is the regularization techniques that impose additional restrictions on an admissible solution. Recently the conjugate gradient methods, where the regularization is inherently built in the iterative procedure, have been employed in the solution of inverse heat conduction problems (IHCP) and found to be very efficient [4].

Contrary to IHCP, inverse convection problems have not been addressed frequently partly due to their mathematical complexity as compared with the inverse heat conduction. Convective heat transfer is governed by a set of nonlinear partial differential equations such as the continuity equation, the Navier–Stokes equation and the energy equation. Therefore, the convection problems are difficult to solve and very few papers devoted to inverse convection have been published so far. Huang and Özisik [5] considers an inverse problem of determining wall heat flux of linear forced convection in the fully developed channel flow from the temperature measurement in the domain. The velocity field is assumed to be the fully developed parabolic one,

* Corresponding author. Tel.: +82-2-705-8482.

0017-9310/99/$ - see front matter
PII: S0017-9310(99)00100-3

Nomenclature

$d^n(t)$	conjugate direction, Eq. (25)
d_x	half width of the system domain
d_y	half depth of the system domain
$G(t)$	heat source function
$\overline{\mathbf{GX}}^{(1)}$	matrix defined in Eq. (60)
$\overline{\mathbf{GX}}^{(2)}$	matrix defined in Eq. (61)
$\overline{\mathbf{GY}}^{(1)}$	matrix defined in Eq. (62)
$\overline{\mathbf{GY}}^{(2)}$	matrix defined in Eq. (63)
J	performance function, Eq. (11)
MO	number of measurement points
NX	number of cells in the x-direction in the Chebyshev pseudospectral method
NY	number of cells in the y-direction in the Chebyshev pseudospectral method
P	pressure
Pr	Prandtl number
q	adjoint pressure field
R	Rayleigh number
t	time
t_f	final time
T	temperature field
T^*_{cold}	temperature at the boundary
T^*_{hot}	characteristic temperature of the system
T^*_{sys}	average temperature of the system
$\boldsymbol{v}$	velocity field.

Greek symbols

α	thermal expansion coefficient
γ^n	parameter defined in Eq. (26)
$\delta(x)$	Dirac delta function
$\delta_n(x)$	function defined in Eq. (8)
δG	variation of the heat source function
δJ	variation of the performance function J
δP	variation of the pressure field
δT	variation of the temperature field
η	adjoint temperature field
κ	thermal diffusivity
ν	kinematic viscosity
ξ	adjoint velocity field
ρ	optimal step length in the conjugate gradient method, Eq. (31)
σ	noise level, Eq. (70)
τ	$t_f - t$
∇J	gradient of the performance function.

Subscripts

m	measurement point
mCG	modified conjugate gradient.

Superscripts

*	dimensional quantities
†	measured variable.

and only the linear convection–conduction equation is dealt to determine the unknown wall heat flux. Further simplification introduced is the neglect of axial conduction, which makes the governing equation parabolic rather than elliptic. They employed the conjugate gradient method [4], which consists of a direct problem, an adjoint problem and the sensitivity problem, to solve the inverse convection problem. For parabolic or unsteady problems, the adjoint problem does not yield a correct conjugate direction at the end point [6], and Huang and Özisik [5] circumvent this difficulty employing the modified conjugate gradient method [7] in addition to the regular conjugate gradient method.

Moutsoglou [8] investigated a steady, two-dimensional, laminar-free convection flow in a vertical channel. The governing equations are simplified by neglecting the axial diffusion of momentum and heat and further by decoupling the longitudinal and lateral pressure gradients, through which the governing equations are parabolized. He considers the case when the heat flux at one wall is unknown and the temperature for the other insulated wall can be measured. The ill-posedness symptoms of the inverse problems are circumvented by adopting the sequential function specification method which is well suited for parabolic problems.

Prud'homme and Nguyen [9] and Nguyen [10] considered an inverse natural convection problem employing a conjugate gradient method. They adopt the stream function-vorticity formulation to describe the flow field and use the adjoint variable method to determine the conjugate direction. Since they do not employ the modified conjugate gradient method [7] to estimate the final time heat flux, $q(t_f)$, their initial approximation of $q(t_f)$ must be a reasonably accurate one.

In the present work, we consider an inverse natural convection problem of determining the unknown strength of a time-varying heat source in a cavity from the temperature measurement within the flow. The governing equation of the natural convection, the Boussinesq equation, is employed without any simplification to determine the velocity and temperature fields. The inverse problem is posed as an optimization problem which is solved by a conjugate gradient method, employing the adjoint equation to obtain the descent direction. The difficulty of obtaining the correct conju-

gate direction at the end point is overcome by employing the modified conjugate gradient method [5,7]. The advantage of the present algorithm adopted is that no a priori information is needed on the shape of an unknown function, since the solution automatically determines the functional form over the whole time domain. Because the governing equation is not simplified in the present analysis of the inverse natural convection problem, this method can be applied to many different inverse convection problems to yield rigorous results.

2. The system and governing equations

We consider a two-dimensional square domain with a time-varying heat source $G(t)$ located at $(x^\dagger, y^\dagger)$. The inverse problem at hand is the estimation of the unknown function $G(t)$ based on the temperature readings of a thermocouple located inside the domain. Due to the heat source, natural convection is induced. The flow pattern is determined by the heat source function $G(t)$. Since the unsteady temperature field inside the cavity is mainly decided by the fluid flow in the cavity, we try to determine the unknown function $G(t)$ from the unsteady temperature readings of a thermocouple located in the cavity.

We use a superscript asterisk to denote dimensional quantities, and introduce the following dimensionless variables:

$$x = \frac{x^*}{d_x}, \quad y = \frac{y^*}{d_y}, \quad t = \frac{\kappa t^*}{d_y^2}, \quad \boldsymbol{v} = \frac{d_y \boldsymbol{v}^*}{\kappa}, \quad T = \frac{T^* - T^*_{\text{cold}}}{T^*_{\text{hot}} - T^*_{\text{cold}}}, \quad P' = \frac{d_y^2 P^*}{\rho \kappa^2} \tag{1}$$

where T^* is the temperature, T^*_{cold} is the temperature at the boundary, T^*_{hot} is the characteristic temperature of the system, t^* is time, $\boldsymbol{v}^*$ is the velocity field, P^* is the pressure field. κ is the thermal diffusivity, ρ is the density, d_x is the half width of the cavity and d_y is the half depth of the cavity. We denote the dimensional heat generation per unit volume per time as $G^*(t^*)\delta_n(x^* - x^{*\dagger})\delta_n(y^* - y^{*\dagger})$, where $(x^\dagger, y^\dagger)$ is the location of the heat source. Then the set of governing equations in dimensionless variables are:

$$\nabla \cdot \boldsymbol{v} = 0 \tag{2}$$

$$\frac{\partial \boldsymbol{v}}{\partial t} + \boldsymbol{v} \cdot \nabla \boldsymbol{v} = -\nabla P + Pr\, \nabla^2 \boldsymbol{v} + R\, Pr\, T\boldsymbol{j} \tag{3}$$

$$\frac{\partial T}{\partial t} + \boldsymbol{v} \cdot \nabla T = \nabla^2 T + G(t)\delta_n(x - x^\dagger)\delta_n(y - y^\dagger) \tag{4}$$

where P is the modified pressure given by:

$$P = P' - (T^*_{\text{cold}} - T^*_{\text{sys}})\frac{d_y^3}{\kappa^2}\alpha g y \tag{5a}$$

and α is the thermal coefficient. Here T^*_{sys} is the average temperature of the system given by;

$$T^*_{\text{sys}} = \tfrac{1}{2}(T^*_{\text{hot}} + T^*_{\text{cold}}) \tag{5b}$$

The dimensionless group R is the Rayleigh number and Pr is the Prandtl number defined as follows:

$$R = \alpha g \frac{(T^*_{\text{hot}} - T^*_{\text{cold}})d_y^3}{\kappa \nu} \tag{5c}$$

$$Pr = \frac{\nu}{\kappa} \tag{5d}$$

where ν is the kinematic viscosity. The dimensionless strength of the heat source $G(t)$ is related to the dimensional strength $G^*(t^*)$ as follows:

$$G(t) = \frac{G^*(t^*)d_y}{(T^*_{\text{hot}} - T^*_{\text{cold}})k d_x} \tag{6a}$$

where k is the thermal conductivity. The characteristic temperature of the system T^*_{hot} is related to the characteristic magnitude of the dimensional heat source G^*_{sys} by the following equation

$$T^*_{\text{hot}} - T^*_{\text{cold}} = \frac{G^*_{\text{sys}}}{k} \tag{6b}$$

Eqs. (5c) and (6b) yield another expression for the Rayleigh number;

$$R = \alpha g \frac{d_y^3 G^*_{\text{sys}}}{\kappa \nu k} \tag{7}$$

The function $\delta_n(x)$, which approximates the point source in the domain, is defined by:

$$\delta_n(x - x^\dagger) = \frac{n}{2\ \cosh^2(n(x - x^\dagger))} \tag{8}$$

and becomes the Dirac delta function as n approaches infinity. In the present work, we take $n = 20$ with $(x^\dagger, y^\dagger) = (0.75, -0.75)$. The shape and strength of the point source $\delta_{20}(x - x^\dagger)\delta_{20}(y - y^\dagger)$ is plotted in Fig. 1, together with the grid system (20×20) employed in the numerical computation. In the same figure, we also plot a typical flow pattern of natural convection arising in the present investigation and indicate the reference location of the temperature measurement point using a small circle. The relevant initial and boundary conditions are

$$t = 0, \quad \boldsymbol{v} = 0, \quad T = 0 \tag{9}$$

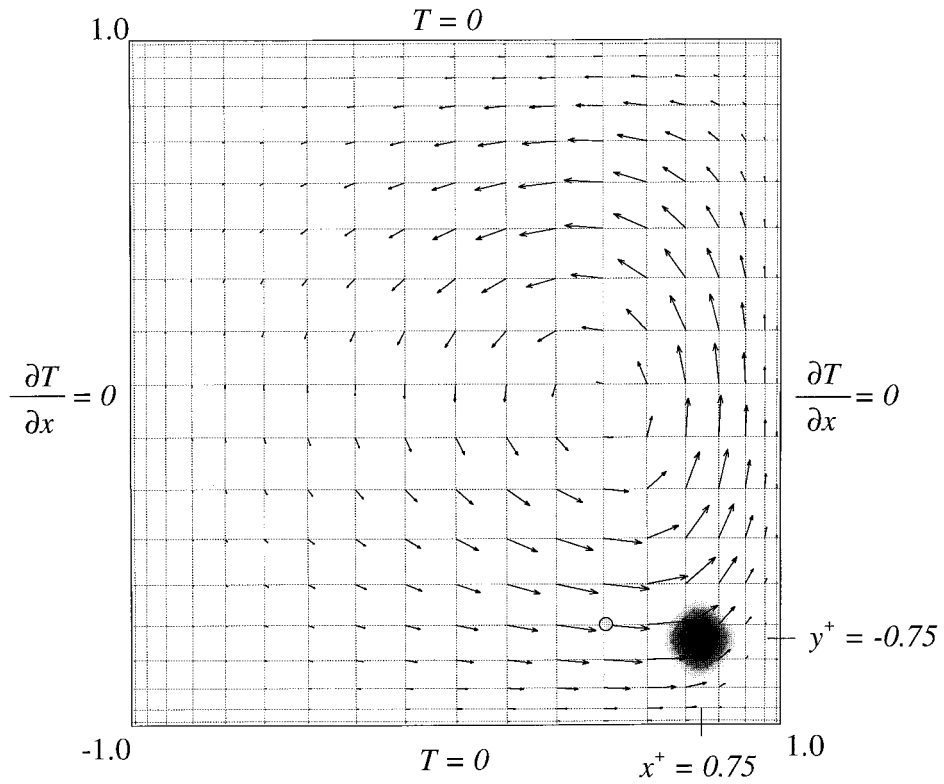

Fig. 1. The system and location of the function $\delta_{20}(x-x^{\dagger})\delta_{20}(y-y^{\dagger})$. The strength of the source is indicated by the degree of darkness. A small circle near the source denotes the reference location of the thermocouple.

$$x = \pm 1, \quad \boldsymbol{v} = 0, \quad \frac{\partial T}{\partial x} = 0 \tag{10a}$$

$$y = \pm 1, \quad \boldsymbol{v} = 0, \quad T = 0 \tag{10b}$$

3. The inverse natural convection problem

The temperature field inside the domain, which can be easily measured at various locations, is determined by the heat source function $G(t)$. Therefore, $G(t)$ can be estimated by using the measured values of the temperature field at certain locations. The performance function for the identification of $G(t)$ is expressed by the sum of square residuals between the calculated and observed temperatures as follows:

$$J = \frac{1}{2}\sum_{m=1}^{MO}\int_0^{t_f} [T(x_m, y_m, t) - T^{\dagger}(x_m, y_m, t)]^2 \, \mathrm{d}t \tag{11}$$

where $T(x_m, y_m, t)$ is the calculated temperature, $T^{\dagger}(x_m, y_m, t)$ is the observed temperature at the location (x_m, y_m), and MO is the total number of measurement points. Although only one measurement point is employed in the present work (i.e., $MO = 1$), summation over the measurement points is kept to make the formula more general. To minimize the performance function (11), we need the gradient of J, ∇J, which is defined by

$$\delta J(G) \equiv J(G + \delta G) - J(G) = \langle \nabla J, \delta G \rangle = \int_0^{t_f} \nabla J \delta G \, \mathrm{d}t \tag{12}$$

where t_f, the final time, is 1.0. The function ∇J can be obtained by introducing the adjoint variables $\boldsymbol{\xi}$, q and η such that the performance function can be rewritten as follows:

$$J(G) = \frac{1}{2}\sum_{m=1}^{MO}\int_0^{t_f} [T(x_m, y_m, t) - T^{\dagger}(x_m, y_m, t)]^2 \, \mathrm{d}t$$

$$-\int_0^{t_f}\int_{\Omega} \boldsymbol{\xi}\left[\frac{\partial \boldsymbol{v}}{\partial t} + \boldsymbol{v}\cdot\nabla\boldsymbol{v} + \nabla P - Pr\,\nabla^2\boldsymbol{v}\right.$$

$$\left. - R\,Pr\,T\boldsymbol{j}\right]\mathrm{d}\Omega\,\mathrm{d}t + \int_0^{t_f}\int_{\Omega} q[\nabla\cdot\boldsymbol{v}]\,\mathrm{d}\Omega\,\mathrm{d}t$$

$$-\int_0^{t_f}\int_\Omega \eta\left[\frac{\partial T}{\partial t}+\boldsymbol{v}\cdot\nabla T-\nabla^2 T\right.$$

$$\left.-G(t)\delta_n(x-x^\dagger)\delta_n(y-y^\dagger)\right]\mathrm{d}\Omega\,\mathrm{d}t \tag{13}$$

The variation of J, δJ, is then given by the following equation:

$$\delta J=\sum_{m=1}^{MO}\int_0^{t_f}[T(x_m,y_m,t)-T^\dagger(x_m,y_m,t)]$$

$$\cdot\delta T(x_m,y_m,t)\,\mathrm{d}t-\int_0^{t_f}\int_\Omega \boldsymbol{\xi}\left[\frac{\partial\delta\boldsymbol{v}}{\partial t}+\delta\boldsymbol{v}\cdot\nabla\boldsymbol{v}\right.$$

$$+\boldsymbol{v}\cdot\nabla\delta\boldsymbol{v}+\nabla\delta P-Pr\,\nabla^2\delta\boldsymbol{v}$$

$$\left.-R\,Pr\,\delta T\boldsymbol{j}\right]\mathrm{d}\Omega\,\mathrm{d}t+\int_0^{t_f}\int_\Omega q[\nabla\cdot\delta\boldsymbol{v}]\mathrm{d}\Omega\,\mathrm{d}t$$

$$-\int_0^{t_f}\int_\Omega \eta\left[\frac{\partial}{\partial t}\delta T+\delta\boldsymbol{v}\cdot\nabla T+\boldsymbol{v}\cdot\nabla\delta T-\nabla^2\delta T\right.$$

$$\left.-\delta G(t)\delta_n(x-x^\dagger)\delta_n(y-y^\dagger)\right]\mathrm{d}\Omega\,\mathrm{d}t \tag{14}$$

Integrating δJ by parts both in space and time, and exploiting the boundary conditions for $\boldsymbol{v}$, $\delta\boldsymbol{v}$, T and δT, the gradient of J, ∇J, defined in Eq. (12) is found to be the following:

$$\nabla J=\int_\Omega \eta\delta_n(x-x^\dagger)\delta_n(y-y^\dagger)\,\mathrm{d}\Omega \tag{15}$$

while the adjoint variables $\boldsymbol{\xi}$, q and η must satisfy:

$$\frac{\partial\boldsymbol{\xi}}{\partial t}+\boldsymbol{v}\cdot\nabla\boldsymbol{\xi}=\nabla q-Pr\,\nabla^2\boldsymbol{\xi}+\boldsymbol{\xi}\cdot(\nabla\boldsymbol{v})^{\mathrm{T}}+\eta\nabla T \tag{16}$$

$$\nabla\cdot\boldsymbol{\xi}=0 \tag{17}$$

$$\frac{\partial\eta}{\partial t}+\boldsymbol{v}\cdot\nabla\eta=-\nabla^2\eta-R\,Pr\,\xi^{y}-\sum_{m=1}^{MO}[T(x,y,t)$$

$$-T^\dagger(x,y,t)]\delta(x-x_m)\delta(y-y_m) \tag{18}$$

where $\delta(x)$ is the diract delta function, superscript 'T' in Eq. (16) means the transpose and $\boldsymbol{\xi}=(\xi^x,\xi^y)$. The relevant boundary conditions are

$$x=\pm1,\quad \boldsymbol{\xi}=0,\quad \frac{\partial\eta}{\partial x}=0 \tag{19}$$

$$y=\pm1,\quad \boldsymbol{\xi}=0,\quad \eta=0 \tag{20}$$

The starting conditions are:

$$\boldsymbol{\xi}(\boldsymbol{x},t=t_f)=0,\quad \eta(\boldsymbol{x},t=t_f)=0 \tag{21}$$

For the convenience of numerical integration, we change the time variable and rewrite Eqs. (16) and (18) as follows:

$$\frac{\partial\boldsymbol{\xi}}{\partial\tau}-\boldsymbol{v}\cdot\nabla\boldsymbol{\xi}=-\nabla q+Pr\,\nabla^2\boldsymbol{\xi}-\boldsymbol{\xi}\cdot(\nabla\boldsymbol{v})^{\mathrm{T}}-\eta\nabla T \tag{22}$$

$$\frac{\partial\eta}{\partial\tau}-\boldsymbol{v}\cdot\nabla\eta=\nabla^2\eta+R\,Pr\,\xi^{y}+\sum_{m=1}^{MO}[T(x,y,t)$$

$$-T^\dagger(x,y,t)]\delta(x-x_m)\delta(y-y_m) \tag{23}$$

where $\tau\equiv t_f-t$ and t_f is the final time.

The Fletcher–Reeves method [11], which is one of the conjugate gradient methods, is successfully applied to the minimization of the performance function, using the gradient of J determined by Eq. (15). The search direction or the conjugate direction at the first step is determined by:

$$d^0(t)=\nabla J(t)=\int_\Omega \eta\delta_n(x-x^\dagger)\delta_n(y-y^\dagger)\,\mathrm{d}\Omega \tag{24}$$

Beginning the second iteration step, the conjugate direction is given by

$$d^n(t)=\nabla J^n(t)+\gamma^n d^{n-1}(t) \tag{25}$$

where

$$\gamma^n=\frac{\displaystyle\int_{t=0}^{t_f}(\nabla J^n(t))^2\,\mathrm{d}t}{\displaystyle\int_{t=0}^{t_f}(\nabla J^{n-1}(t))^2\,\mathrm{d}t} \tag{26}$$

and n is the iteration number. Once the conjugate direction is obtained, the heat source function $G(t)$ is updated in that direction.

$$G^{n+1}(t)=G^n(t)-\rho d^n(t) \tag{27}$$

The optimal step length ρ in the direction $d^n(t)$ is obtained by minimizing $J(G^n-\rho d^n)$ with respect to ρ. Formally, $J(G^n-\rho d^n)$ is expressed as:

$$J(G^n-\rho d^n)=\frac{1}{2}\int_0^{t_f}\sum_{m=1}^{MO}[T(x_m,y_m;G^n-\rho d^n)$$

$$-T^\dagger(x_m,y_m,t)]^2\,\mathrm{d}t \tag{28}$$

The directional derivative of T at $G(t)$ in the direction of $d(t)$, denoted as δT, is defined by

$$\delta T=\lim_{\epsilon\to0}\frac{T(G+\epsilon d)-T(G)}{\epsilon} \tag{29}$$

Then, the term $T(x_m,y_m;G^n-\rho d^n)$ in Eq. (28) is approximated by

$$T(x_m,y_m;G^n-\rho d^n)=T(x_m,y_m;G^n)$$

$$-\delta T(x_m,y_m,t)\rho \tag{30}$$

Substituting Eq. (30) into Eq. (28), partially differentiating it with respect to ρ and setting the resulting equation equal to zero, the value of ρ that minimizes $J(G^n-\rho d^n)$ is obtained as

$$\rho = \frac{\delta J^n}{K^n} \tag{31}$$

where

$$K^n = \sum_{m=1}^{MO}\int_0^{t_f} [\delta T(x_m, y_m, t)]^2 \, \mathrm{d}t \tag{32}$$

and

$$\delta J^n = \sum_{m=1}^{MO}\int_0^{t_f} [T(x_m, y_m, t) - T^{\dagger}(x_m, y_m, t)]\delta T(x_m, y_m, t) \, \mathrm{d}t \tag{33}$$

The sensitivity equation which determines δT is given by the following set of equations

$$\nabla \cdot \delta \boldsymbol{v} = 0 \tag{34}$$

$$\frac{\partial}{\partial t}\delta \boldsymbol{v} + \delta \boldsymbol{v} \cdot \nabla \boldsymbol{v}\, \boldsymbol{v} \cdot \nabla \delta \boldsymbol{v} = -\nabla \delta P + Pr\, \nabla^2 \delta \boldsymbol{v} + R\, Pr\, \delta T \boldsymbol{j} \tag{35}$$

$$\frac{\partial}{\partial t}\delta T + \delta \boldsymbol{v} \cdot \nabla T + \boldsymbol{v} \cdot \nabla \delta T = \nabla^2 \delta T + d(t)\delta_n(x - x^{\dagger})\delta_n(y - y^{\dagger}) \tag{36}$$

The relevant initial and boundary conditions for the set of sensitivity equations are

$$t = 0, \quad \delta \boldsymbol{v}(x, y, t = 0) = 0, \quad \delta T(x, y, t = 0) = 0 \tag{37}$$

$$x = \pm 1, \quad \delta \boldsymbol{v} = 0, \quad \frac{\partial}{\partial x}\delta T = 0 \tag{38}$$

$$y = \pm 1, \quad \delta \boldsymbol{v} = 0, \quad \delta T = 0 \tag{39}$$

The present algorithm of the conjugate gradient method is summarized as follows:

1. Assume the heat source function $G(t)$ and calculate the velocity and temperature fields by solving Eqs. (2)–(10).
2. Solve the adjoint Eqs. (17), (19)–(23) from $\tau = 0$ to $\tau = t_f$.
3. ∇J is determined by Eq. (15).
4. The conjugate direction $d^n(t)$ is given by Eq. (25) with γ^n determined by Eq. (26).
5. Solve the sensitivity Eqs. (34)–(39).
6. The optimal step length in the conjugate direction $d^n(t)$ is determined by Eq. (31).
7. The heat source function $G(t)$ is updated according to Eq. (27).
8. Repeat the above procedure until convergence.

4. Modified conjugate gradient approach [5,7]

Although the conjugate gradient method employing the adjoint equation, as described in the previous section, yields the converged profile of the heat source function in a short time, the estimated value of the heat source function at the final time, $G(t_f)$, will always be equal to the initial guess $G^0(t_f)$. The reason for this is obvious from Eqs. (15), (21), (25) and (27). Since the value of $\eta(\boldsymbol{x}, t)$ is zero at the final time, $t = t_f$, the gradient of the performance function, ∇J, is also zero at $t = t_f$ due to Eq. (15). This causes the conjugate direction $d(t)$ to vanish at $t = t_f$ [cf Eq. (25)], and consequently, leaves the heat source function at the final time $G(t_f)$ remaining at its initial guess $G^0(t_f)$. This difficulty with the conjugate gradient method employing the adjoint equation usually arises in the parabolic equations as well as the unsteady equations. The difficulty encountered at the final time t_f can be alleviated by the following modified conjugate gradient method. We seek a continuously differentiable function $G(t)$ such that

$$G(t) = \int_a^t \frac{\mathrm{d}G(t')}{\mathrm{d}t'} \, \mathrm{d}t' \tag{40}$$

From Eqs. (12) and (15), the variation of the performance function δJ may be rewritten as:

$$\delta J = \int_0^{t_f} \delta G(t) \int_\Omega \eta(x, y, t)\delta_{20}(x - x^{\dagger})\delta_{20}(y - y^{\dagger}) \, \mathrm{d}\Omega \, \mathrm{d}t \tag{41}$$

If Eq. (41) is integrated by parts with respect to a time variable, we find that

$$\delta J = -\int_0^{t_f} \frac{\mathrm{d}\delta G}{\mathrm{d}t} \int_{t_f}^{t} \int_\Omega \eta(x, y, t')\delta_{20}(x - x^{\dagger}) \delta_{20}(y - y^{\dagger}) \mathrm{d}\Omega \, \mathrm{d}t' \, \mathrm{d}t \tag{42}$$

Therefore, the derivative of J with respect to $\mathrm{d}G/\mathrm{d}t$ is given by the following expression.

$$\nabla J\left(\frac{\mathrm{d}G}{\mathrm{d}t}\right) = -\int_{t_f}^{t} \int_\Omega \eta(x, y, t')\delta_{20}(x - x^{\dagger}) \delta_{20}(y - y^{\dagger}) \mathrm{d}\Omega \, \mathrm{d}t' \tag{43}$$

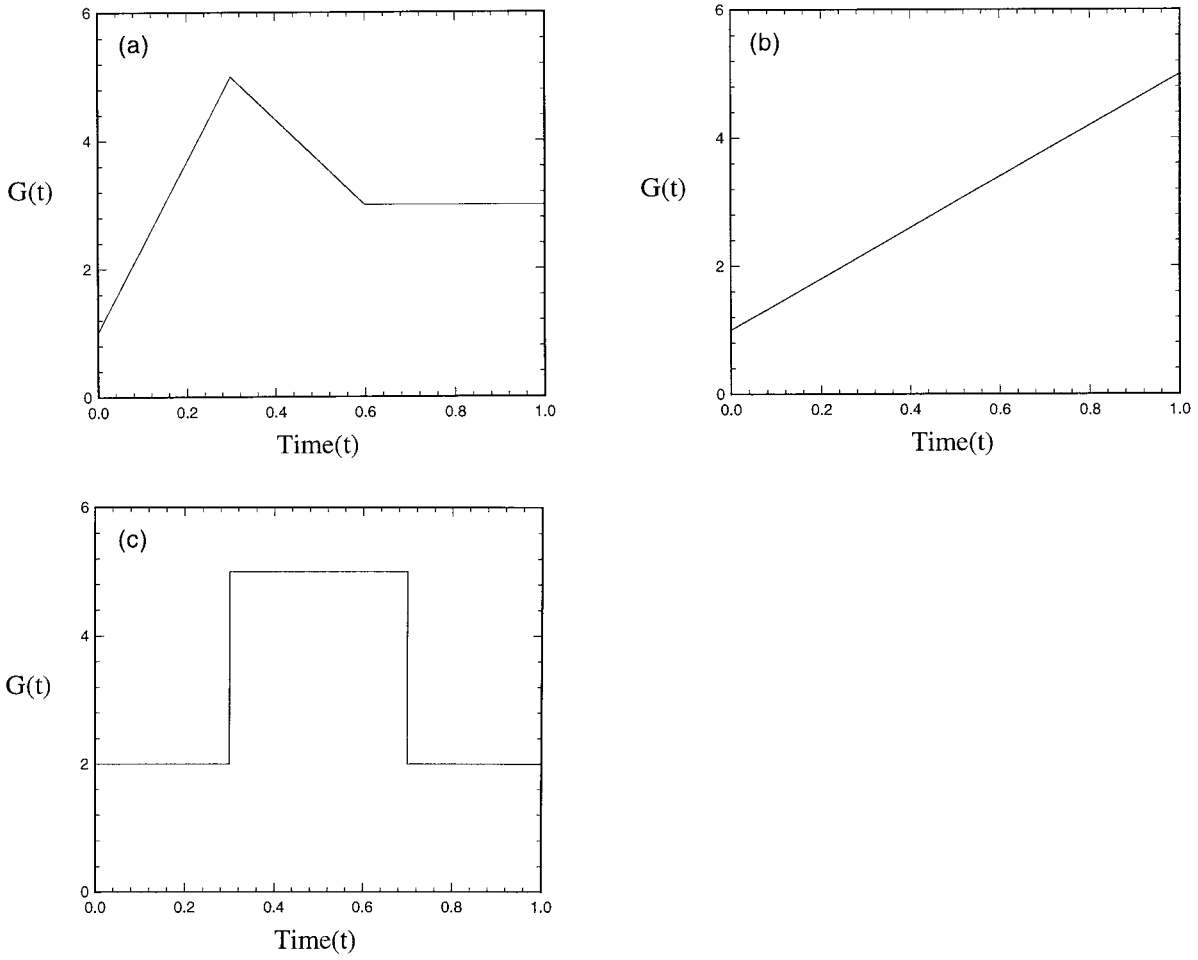

Fig. 2. (a–c) Various shapes of the heat source function considered in the present investigation.

Then, we take the conjugate direction as follows:

$$d^n(t) = \int_0^t D^n(t')\,\mathrm{d}t' \tag{44}$$

where

$$D^n = \nabla J\left(\frac{\mathrm{d}G}{\mathrm{d}t}\right)^n + \gamma^n D^{n-1} \tag{45}$$

Since $d_n(t_f)$, obtained by Eq. (44), is nonzero, the modified conjugate gradient method yields a reasonably accurate value of $G(t_f)$ contrary to the previous regular conjugate gradient method. On the other hand, from Eq. (44) it can be seen that $d^n(0)=0$. Then, for the same reason with the regular conjugate gradient method, the modified conjugate gradient method will not improve the starting value $G(0)$. In the present work, this dilemma is overcome by combining the regular and modified conjugate gradient method sequentially. At the first stage, we employ the modified conjugate gradient method for a certain number of iterations until a reasonably good estimation of the end value $G(t_f)$ is attained. Afterwards, the regular conjugate gradient method is adopted using the estimation of the modified conjugate gradient method as the initial approximation until a converged profile is obtained.

5. The Chebyshev pseudospectral method

The sets of equations governing the present problem of inverse natural convection, i.e., the set of Eqs. (2)–(10) for the direct problem, the set of Eqs. (17), (19)–(23) for the adjoint problem and the set of Eqs. (34)–(39) for the sensitivity problem, are solved by employing the following time splitting scheme to impose the

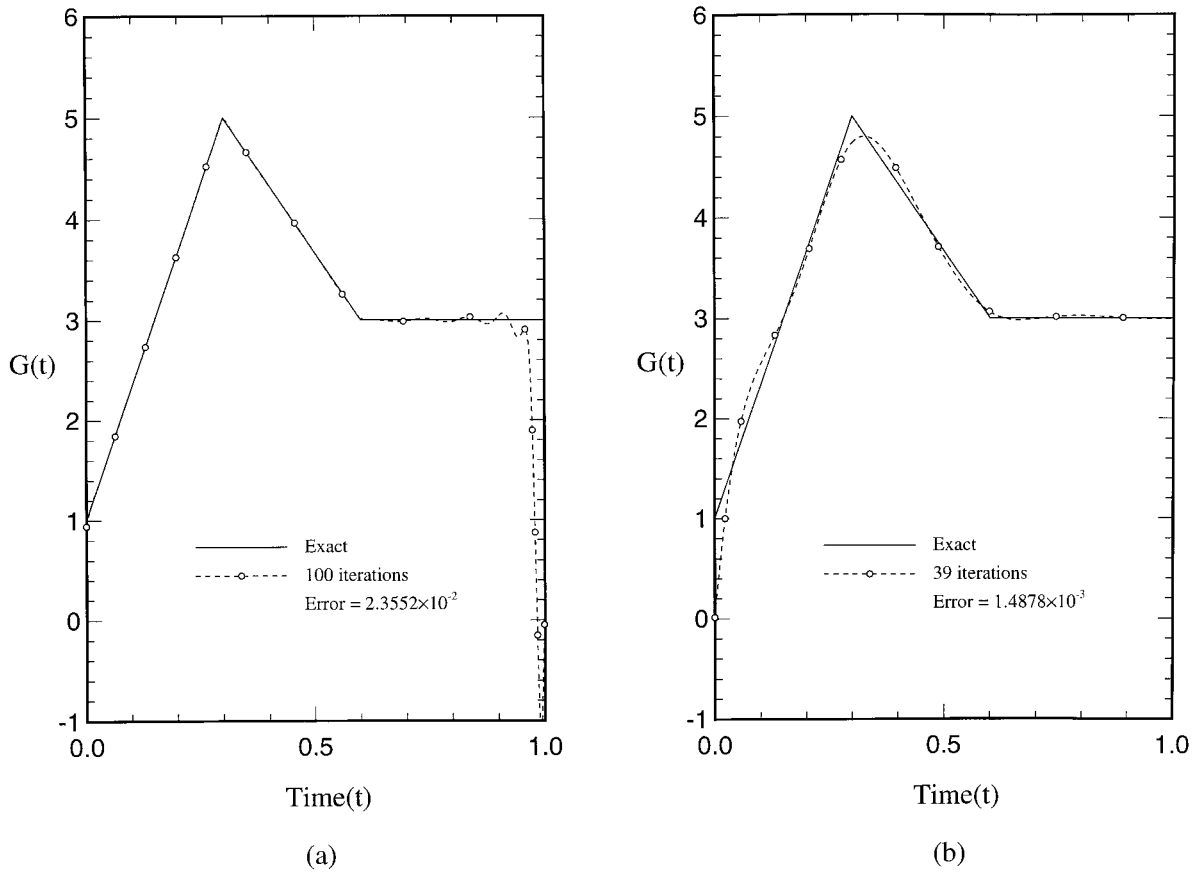

Fig. 3. The estimated profiles of the heat source function. (a) Regular conjugate gradient method. (b) Modified conjugate gradient method.

solenoidal conditions, Eqs. (2), (17) and (34), implicitly.

5.1. Direct problem

Prediction step

$$\frac{\boldsymbol{v}^* - \boldsymbol{v}^n}{\Delta t} = -\boldsymbol{v}^n \cdot \nabla \boldsymbol{v}^n + Pr\,\nabla^2 \boldsymbol{v}^n + R\,Pr\,T^n \boldsymbol{j} \tag{46}$$

Pressure equation

$$\nabla^2 P^{n+1} = \frac{1}{\Delta t} \nabla \cdot \boldsymbol{v}^* \tag{47}$$

Correction step

$$\frac{\boldsymbol{v}^{n+1} - \boldsymbol{v}^*}{\Delta t} = -\nabla P^{n+1} \tag{48}$$

Energy equation

$$\frac{T^{n+1} - T^n}{\Delta t} = -\boldsymbol{v}^{n+1} \cdot \nabla T^{n+1} + \nabla^2 T^{n+1} + G(t^{n+1})\delta_{20}(x - x^\dagger)\delta_{20}(y - y^\dagger) \tag{49}$$

5.2. Adjoint equation

Prediction step

$$\frac{\xi^* - \xi^l}{\Delta \tau} = \boldsymbol{v}^l \cdot \nabla \xi^l + Pr\,\nabla^2 \xi^l - \xi^l \cdot (\nabla \boldsymbol{v}^l)^{\mathrm{T}} - \eta \nabla T^l \tag{50}$$

Pressure equation

$$\nabla^2 q^{l+1} = \frac{1}{\Delta \tau} \nabla \cdot \xi^* \tag{51}$$

Correction step

$$\frac{\xi^{l+1} - \xi^*}{\Delta \tau} = -\nabla q^{l+1} \tag{52}$$

Energy adjoint equation

$$\frac{\eta^{l+1}-\eta^{l}}{\Delta\tau}=\boldsymbol{v}^{l+1}\cdot\nabla\eta^{l+1}+\nabla^2\eta^{l+1}+R\,Pr(\xi^{y})^{l+1}$$

$$+\sum_{m=1}^{MO}[T^{l+1}-(T^{\dagger})^{l+1}]\delta(x-x_m)\delta(y-y_m) \tag{53}$$

5.3. Sensitivity equation

Prediction step

$$\frac{\delta\boldsymbol{v}^{*}-\delta\boldsymbol{v}^{n}}{\Delta t}=-\delta\boldsymbol{v}^{n}\cdot\nabla\boldsymbol{v}^{n}-\boldsymbol{v}^{n}\cdot\nabla\delta\boldsymbol{v}^{n}+Pr\,\nabla^2\delta\boldsymbol{v}^{n}+R\,Pr\,\delta T^{n}\boldsymbol{j} \tag{54}$$

Pressure equation

$$\nabla^2\delta P^{n+1}=\frac{1}{\Delta t}\nabla\cdot\delta\boldsymbol{v}^{*} \tag{55}$$

Correction step

$$\frac{\delta\boldsymbol{v}^{n+1}-\delta\boldsymbol{v}^{*}}{\Delta t}=-\nabla\delta P^{n+1} \tag{56}$$

Energy sensitivity equation

$$\frac{\delta T^{n+1}-\delta T^{n}}{\Delta t}=$$

$$-\delta\boldsymbol{v}^{n+1}\cdot\nabla T^{n+1}-\boldsymbol{v}^{n+1}\cdot\nabla\delta T^{n+1}+\nabla^2\delta T^{n+1}$$

$$+d(t^{n+1})\delta_{20}(x-x^{\dagger})\delta_{20}(y-y^{\dagger}) \tag{57}$$

The discretization of the spatial derivatives in Eqs. (46)–(57) is performed by using the Chebyshev pseudospectral method [12]. Adoption of this technique allows one to approximate differentiation of a function with matrix multiplication. According to the Chebyshev pseudospectral method the collocation points are selected as:

$$x_i=\cos\left[\frac{\pi(i-1)}{NX}\right]\quad(1\le i\le NX+1) \tag{58}$$

$$y_j=\cos\left[\frac{\pi(j-1)}{NY}\right]\quad(1\le j\le NY+1) \tag{59}$$

where NX and NY are the number of computational cells in the x- and y-direction, respectively. Then the

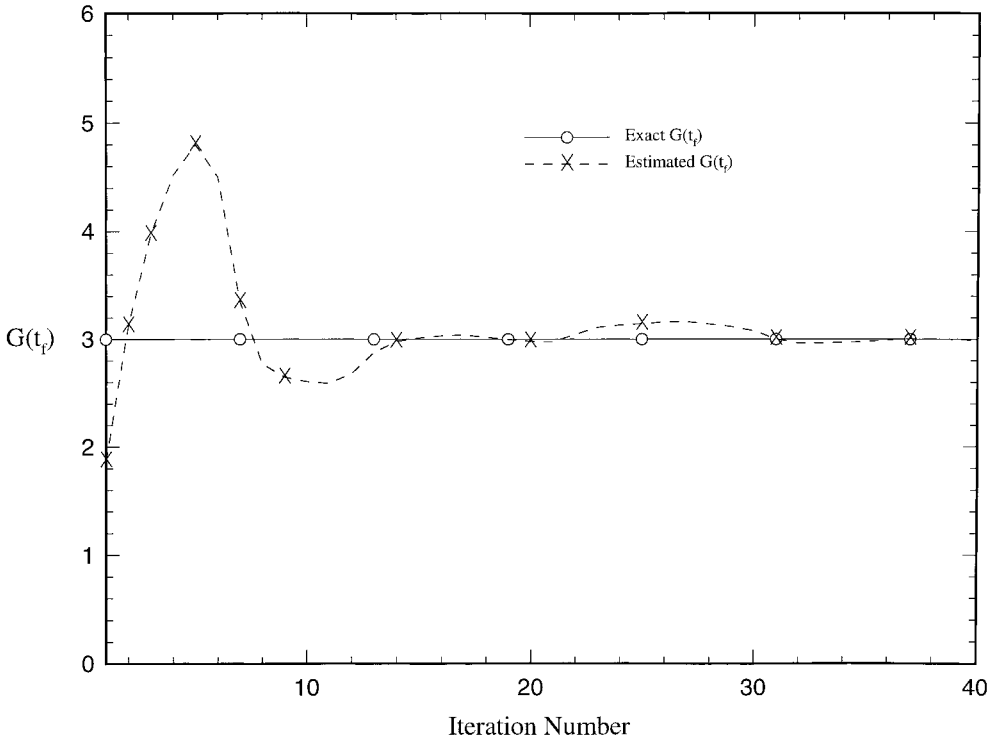

Fig. 4. The convergence of the end point value $G(t_f)$ with respect to the iteration number for Case (a) of Fig. 2 when using the modified conjugate gradient method.

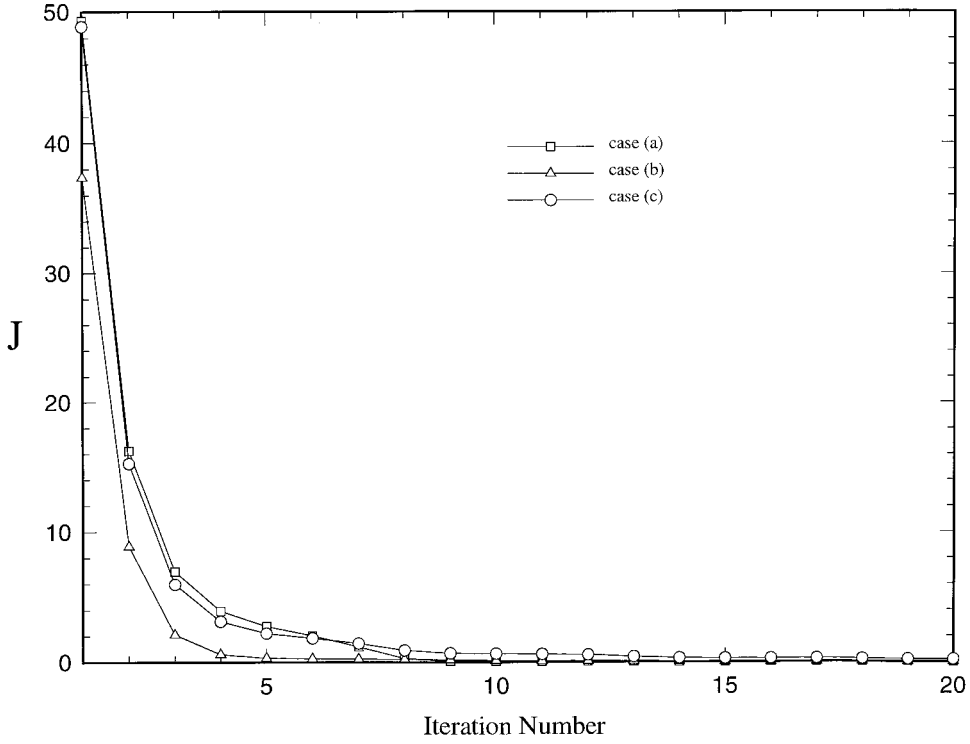

Fig. 5. The rate of minimization of the performance function J when employing the combined iteration scheme.

first and second partial derivatives of a function $u(x, y)$, defined for $-1 \le x \le 1$ and $-1 \le y \le 1$, can be approximated by:

$$\frac{\partial u}{\partial x}(x_i, y_j) = \sum_{l=1}^{NX+1} \tilde{G}X_{il}^{(1)} u(x_l, y_j) \tag{60}$$

$$\frac{\partial^2 u}{\partial x^2}(x_i, y_j) = \sum_{l=1}^{NX+1} \tilde{G}X_{il}^{(2)} u(x_l, y_j) \tag{61}$$

$$\frac{\partial u}{\partial y}(x_i, y_j) = \sum_{l=1}^{NY+1} \tilde{G}Y_{jl}^{(1)} u(x_i, y_l) \tag{62}$$

$$\frac{\partial^2 u}{\partial y^2}(x_i, y_j) = \sum_{l=1}^{NY+1} \tilde{G}Y_{jl}^{(2)} u(x_i, y_l) \tag{63}$$

The detailed expressions for the matrices $\overline{\mathbf{GX}}^{(1)}$, $\overline{\mathbf{GX}}^{(2)}$, $\overline{\mathbf{GY}}^{(1)}$ and $\overline{\mathbf{GY}}^{(2)}$, are given in Ku et al. [12]. Numerical inversion of large matrices arising in Eqs. (47), (49), (51), (53), (55) and (57) has been done by the tensor-product method.

6. Results

The accuracy of the present inverse analysis is examined for estimating the unknown strength of a time-varying heat source $G(t)$ in the domain. Several test cases have been run with simulated measurements $T^{\dagger}(x_m, y_m, t)$, and the estimated strength of the heat source is compared with the exact one. The grid system adopted is (20×20), which is found to be sufficient to resolve the flow and temperature fields when $d_x = 1$ cm, $d_y = 0.5$ cm, thermal diffusivity $\kappa = 2.06 \times 10^{-5}$ m^2/s, $\alpha = 3.36 \times 10^{-3}$ K^{-1} and the Prandtl number $Pr = 0.72$. The corresponding Rayleigh number is about 4000. We consider three different cases of heat source functions $G(x)$, as depicted in Figs. 2(a–c). The minimization of the performance function, Eq. (11), is done by the conjugate gradient method of Fletcher and Reeves [11], where the initial approximation of $G(t)$ is taken to be 0.0 (constant) for all numerical experiments described below. The equation of $G(t)$ for

the three cases shown in Fig. 2 are as follows:

(a) $G(t) = \frac{4}{0.3}t + 1 \quad (0 \le x \le 0.3)$

$G(t) = -\frac{2}{0.3}t + 7 \quad (0.3 \le x \le 0.6)$

$G(t) = 3.0 \quad (0.6 \le x \le 1)$ (64)

(b) $G(t) = 4t + 1 \quad (0 \le x \le 1)$ (65)

(c) $G(t) = 2.0 \quad (0 \le x \le 0.3)$

$G(t) = 5.0 \quad (0.3 \le x \le 0.7)$

$G(t) = 2.0 \quad (0.7 \le x \le 1)$ (66)

The accuracy of the estimation is quantified by the following definition of estimation error:

$$\text{Error} = \frac{\|G_{\text{estimated}} - G_{\text{exact}}\|_{L_2}^2}{\|G_{\text{exact}}\|_{L_2}^2} \quad (67)$$

where $\|\cdot\|_{L_2}$ is the usual L_2-norm. The simulated measurements containing measurement errors are generated by adding random errors to the computed exact temperatures as follows:

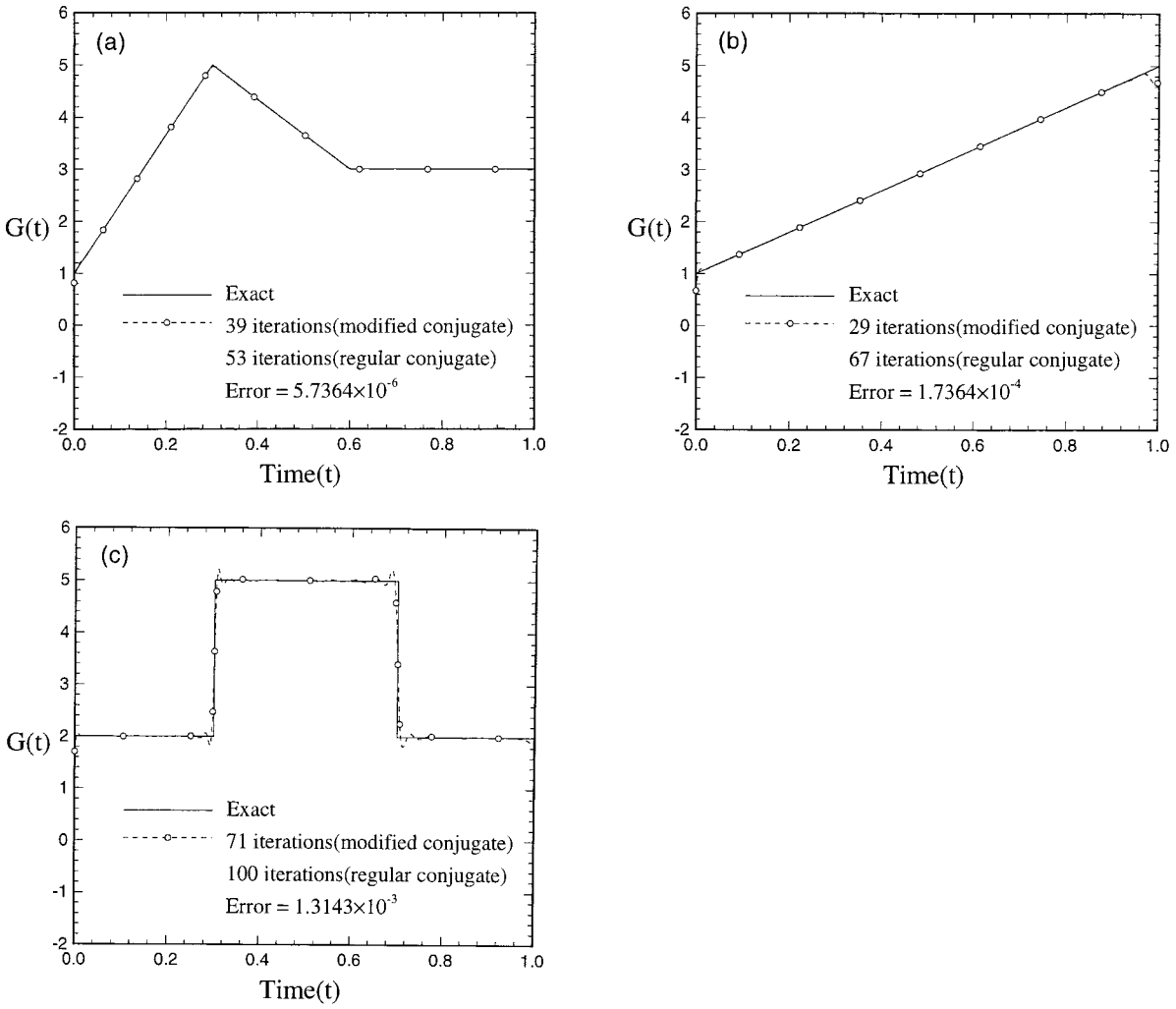

Fig. 6. The estimated profiles of the heat source function $G(t)$ when the combined iteration scheme is employed. The iteration number of the modified conjugate gradient technique and that of the regular conjugate gradient technique are indicated as well as the estimation error. (a) Case (a) of Fig. 2. (b) Case (b) of Fig. 2. (c) Case (c) of Fig. 2.

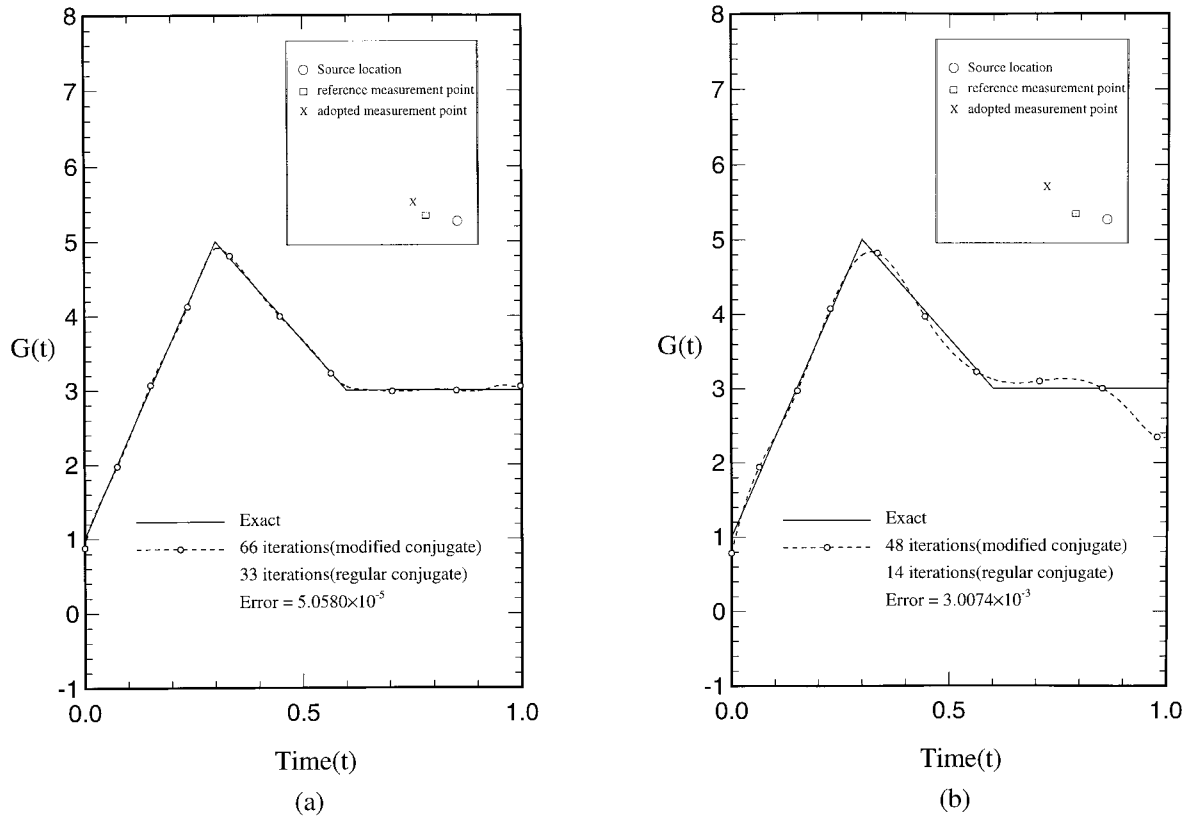

Fig. 7. The effect of the location of the measurement point (x^*, y^*) on the accuracy of the estimation. The locations of the heat source, reference measurement point and the adopted measurement point are indicated in small boxes inserted. (a) (x^*, y^*) = (0.3090, −0.5878). (b) (x^*, y^*) = (0.1564, −0.4540).

$$T_{\text{measured}}(= T^{\dagger}) = T_{\text{exact}} + \omega\sigma \tag{68}$$

where σ determines the noise level, which takes values of 0.0, 0.05, 0.1, and ω is a random number between $-2.576 \le \omega \le 2.576$. In fact, σ is the standard deviation of measurement errors which are assumed to be the same for all measurements, and ω is the Gaussian distributed random error. The above range of the ω value corresponds to the 99% confidence bound for the temperature measurement. Specifically, $\sigma = 0.05$ corresponds to about 3% relative measurement error and $\sigma = 0.1$ induces about 6% relative measurement error.

To check the accuracy of the present algorithm for solving the inverse natural convection problems, we first consider an idealized situation in which there are no measurement errors, i.e., $\sigma = 0.0$. The temperature recordings are assumed to be done continuously by a thermocouple located at the reference position (0.4540, −0.7071) while the source is located at (0.75, −0.75) as shown in Fig. 1. Figs. 3(a) and (b) show the estimated heat source function $G(t)$ for Case (a) when the regular conjugate gradient (Fig. 3(a)) and the modified conjugate gradient method (Fig. 3(b)) are employed. As explained in the previous sections, the regular conjugate gradient method does not improve the end point value $G(t_f)$ while the modified conjugate gradient method has the same difficulty with the starting point value $G(0)$. The combined iteration scheme [6] is employed to overcome this dilemma. At the first stage, we employ the modified conjugate gradient method for a certain number of iterations until a reasonably good estimation of the end poind value $G(t_f)$ is attained. Afterwards, the regular conjugate gradient method is adopted using the estimation of the modified conjugate gradient method as the initial approximation to get the final converged profile. Fig. 4 shows the convergence of the end point value $G(t_f)$ with respect to the iteration number for Case (a) when using the modified conjugate gradient method. The error of $G(t_f)$ with the modified conjugate gradient method is defined by:

$$E_{\text{mCG}} = \sum_{i=1}^{3} \frac{| G^n(t_f) - G^{n-i}(t_f) |}{| G^n(t_f) |} \tag{69}$$

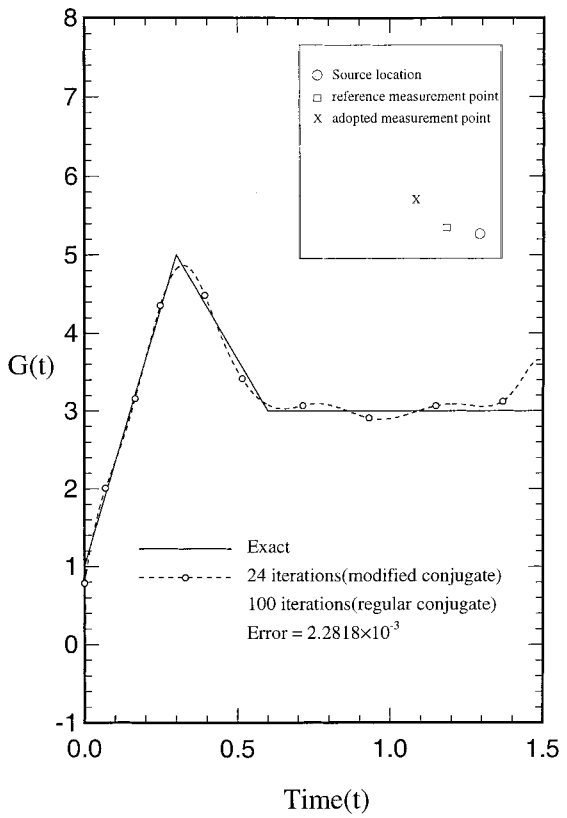

Fig. 8. The effect of the duration of the measurement time on the accuracy of estimation at $t = t_f(1.0)$.

and the iteration of the modified conjugated gradient is stopped when $E_{mCG} < 0.01$.

Fig. 5 plots the rate of minimization of the performance function when the combined iteration scheme is applied to the three cases of Fig. 2. For all three cases investigated, the value of the performance function J is reduced rapidly during the first couple of iterations, but we usually need many more iterations to make the starting point value $G(0)$ and the end point value $G(t_f)$ converge. Figs. 6(a–c) show the estimated profiles of the heat source function $G(t)$ for the three cases of Fig. 2. The estimated profiles are in excellent agreement with the exact heat source function over the whole domain, with the error of the converged profile, determined by Eq. (67), being 5.7364×10^{-4}, 1.7364×10^{-4} and 1.3143×10^{-3}, respectively. The number of iterations in the steps of modified conjugate gradient and regular conjugate gradient are also indicated in the same figure.

Figs. 7(a) and (b) show the effect of the location of a thermocouple on the accuracy of the estimated heat source function. In addition to the previous reference location $(x_m, y_m) = (0.4540, -0.7071)$, we consider two more locations farther from the heat source than the reference one, i.e. (0.3090, −0.5878) and (0.1564, −0.4540). Fig. 7(a) is the estimated profile for Case (a) when the measurement point is at (0.3090, −0.5878) and Fig. 7(b) is the result with the measurement point located at (0.1564, −0.4540). The locations of these new measurement points are indicated in the small boxes inserted in Fig. 7. Comparing the results of Fig. 6(a) with those of Fig. 7, we find that as the location of the thermocouple approaches that of the heat source, the accuracy improves, since the sensitivity of the temperature field with respect to the heat source increases as the distance between the measurement point and the heat source decreases. The noticeable inaccuracy in the estimated profile of $G(t)$ near the final time for the case of Fig. 7(b) is thought to be incurred by the finite speed of information transfer from the heat source to the measurement point. In Fig. 8 we lengthen the measurement time duration from 1.0 to 1.5 so that the thermocouple at the new measurement point could have sufficient time to notice the variation of $G(t)$. The estimated value of $G(t)$ at $t = t_f(1.0)$ is now found to be reasonably accurate.

Next, the effect of noise level on the accuracy of the estimation is investigated. In all practical experimental situations it is expected that some errors will be induced into measurements. The following discrepancy principle is adopted as the stopping criterion for the iterative procedure of the conjugate gradient method when there are measurement errors [5,6]. Assuming the measurement errors to be the same for all thermocouples, i.e.

$$T(x_m, y_m, t) \quad - T^{\dagger}(x_m, y_m, t) \approx \sigma \tag{70}$$

Introducing this result into Eq. (11), we find

$$J \approx \frac{1}{2}\int_0^{t_f} \sum_{m=1}^{MO} \sigma^2 \, dt \equiv \epsilon^2 \tag{71}$$

Then the discrepancy principle for the stopping criterion is taken as

$$J < \epsilon^2 \tag{72}$$

If the function J has a minimum value that is larger than ϵ^2, the following criterion is used to stop the iteration

$$J(G^{(i+1)}) - J(G^{(i)}) < \epsilon_1 \tag{73}$$

where ϵ_1 is a prescribed small number. Figs. 9(a) and (b) are the estimated heat source function for Case (a) of Fig. 2 when the noise level is $\sigma = 0.05$ and 0.1, respectively. As expected, the accuracy of estimation deteriorates as the noise level increases.

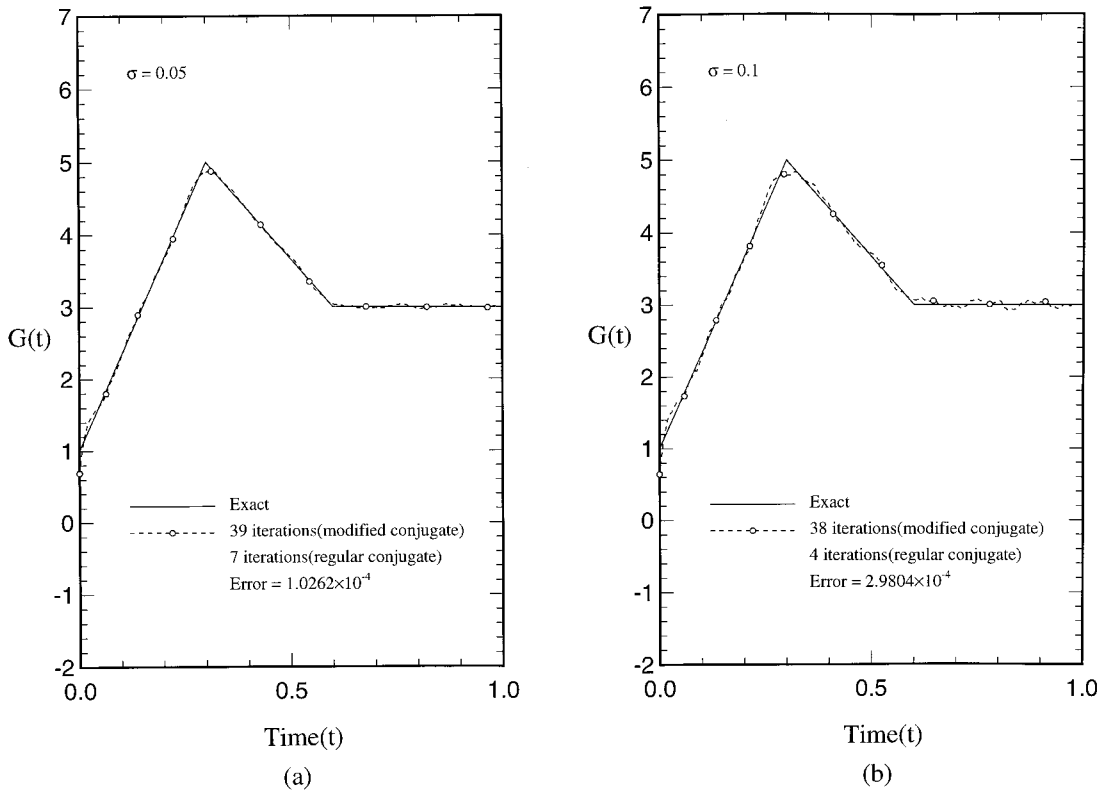

Fig. 9. The effect of the noise level σ on the accuracy of the estimation. (a) $\sigma = 0.05$. (b) $\sigma = 0.1$.

Finally, the effect of the Rayleigh number on the accuracy of the estimation is investigated. As the Rayleigh number increases, the convection pattern becomes more and more complicated. Thus, it is expected that the accuracy of the estimation will deteriorate as the Rayleigh number increases when the same measurement point is employed. Eventually when the Rayleigh number becomes sufficiently large the convection is turned into turbulence, and it will be quite difficult to estimate $G(t)$ employing only one measurement point. Figs. 10(a) and (b) show the estimated profiles of $G(t)$ when the Rayleigh number is 12,000 (Fig. 10(a)) and 20,000 (Fig. 10(b)). Comparing these results with the previous one of the default Rayleigh number 4000 (Fig. 6(a)), it is found that the estimation error increases when the Rayleigh number increases.

7. Conclusion

The inverse natural convection problem of estimating the unknown strength of a time-varying heat source from the temperature measurement within the flow is investigated by employing the conjugate gradient method. Contrary to the previous works on the inverse natural convection problems, the present method employs the exact Boussinesq equation without any simplifications to yield rigorous results. The gradient of the performance function needed in the conjugated gradient technique is obtained by solving the adjoint equation. The conjugate gradient method employing the adjoint equation, though it is computationally very efficient, does not correctly estimate the end point value of the unknown function for unsteady problems as considered in the present work. In the present investigation, this difficulty is overcome by combining the modified conjugate gradient method [5,7] with the regular conjugate gradient method. The present method is found to solve the inverse natural convection problem accurately without a priori information about the unknown function to be estimated.

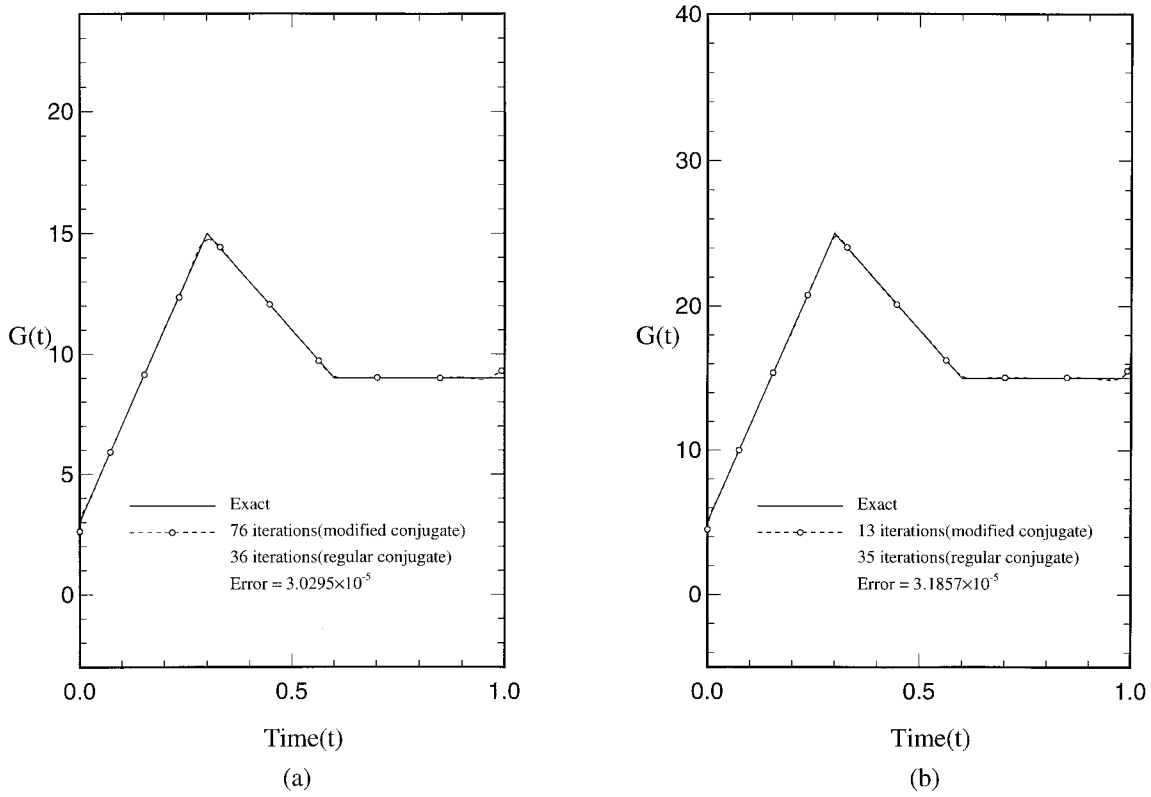

Fig. 10. The effect of the Rayleigh number on the accuracy of the estimation. (a) $R = 12{,}000$. (b) $R = 20{,}000$.

References

[1] J.V. Beck, K.J. Arnold, Parameter Estimation in Engineering and Science, John Wiley and Sons, New York, 1977.

[2] J.V. Beck, B. Blackwell, C.R. St-Clair Jr, Inverse Heat Conduction: Ill-Posed Problems, Wiley-Interscience, New York, 1985.

[3] O.M. Alifanov, Inverse Heat Transfer Problems, Springer-Verlag, Berlin, 1994.

[4] Y. Jarny, M.N. Özisik, J.P. Bardon, A general optimization method using an adjoint equation for solving multidimensional inverse heat conduction, Int. J. Heat Mass Transfer 34 (1991) 2911–2919.

[5] C.H. Huang, M.N. Özisik, Inverse problem of determining unknown wall flux in laminar flow through a parallel plate duct, Num. Heat Transfer, Part A 21 (1992) 55–70.

[6] H.M. Park, O.Y. Chung, J.H. Lee, On the solution of inverse heat transfer problem using the Karhunen–Loève Galerkin method, Int. J. Heat Mass Transfer 42 (1999) 127–142.

[7] O.M. Alifanov, V.V. Mikhailov, Solution of the nonlinear inverse thermal conductivity problem by the iteration method, J. Engng Phys. 35 (1978) 1501–1506.

[8] A. Moutsoglou, An inverse convection problem, ASME J. Heat Transfer 221 (1989) 37–43.

[9] M. Prud'homme, T.H. Nguyen, Whole time-domain approach to the inverse natural convection problem, Num. Heat Transfer, Part A 32 (1997) 169–186.

[10] T.H. Nguyen. Inverse convection problem: a preview, in: Proceedings Sec. Int. Therm. Energy Congress, Agadir, Morroco, 1995, vol. 1, pp. 1–11.

[11] R. Fletcher, R.M. Reeves, Function minimization by conjugate gradients, The Computer Journal 7 (1964) 149–154.

[12] H.C. Ku, T.D. Taylor, R.S. Hirsh, Pseudospectral methods for solution of the incompressible Navier–Stokes equations, Computer and Fluids 15 (1987) 195–214.